Ivabradine promotes angiogenesis and reduces cardiac hypertrophy in mice with myocardial infarction

Xiangqi Wu#, Wei You#, Zhiming Wu, Fei Ye, Shaoliang Chen

Division of Cardiology, Nanjing First Hospital, Nanjing Medical University; Nanjing-*China*

Abstract

Objective: We investigated the underlying mechanism of ivabradine (IVA) in promoting angiogenesis and reducing cardiac hypertrophy in mice with myocardial infarction (MI).

Methods: Nineteen mice were randomly assigned into three groups as follows: sham group (10 ml/kg/day phosphate buffer saline (PBS), n=6), model group (MI and 10 ml/kg/day PBS, n=6) and IVA group (MI and 10 mg/kg/day IVA, n=7). All groups received an intragastric gavage for four weeks. Heart and body mass were measured. Cardiac function and heart rate were assessed by echocardiography and electrocardiography, respectively. The collagen deposition, area of cardiomyocytes, and number of capillaries were evaluated using Masson's staining, anti-wheat germ agglutinin (WGA) staining, and platelet endothelial cell adhesion molecule-1 (CD31) staining, respectively. The protein kinase B (Akt)-endothelial nitric oxide synthase (eNOS) signaling and p-38 mitogen-activated protein kinase (MAPK) family in myocardium were determined by western blot.

Results: IVA treatment greatly improved cardiac dysfunction and suppressed cardiac hypertrophy at 4 weeks after MI ($p<0.05$). Heart rate and fibrotic area of IVA group declined notably compared to those of the model group ($p<0.05$). IVA administration substantially reduced cardiomyocyte size and increased capillary formation ($p<0.05$). Besides, IVA medication can enhance Akt-eNOS signaling and inhibit p38 MAPK phosphorylation in the heart of mice with MI ($p<0.05$).

Conclusion: IVA can perform two functions, the promotion of angiogenesis and the reduction of cardiac hypertrophy, both of which were closely associated with Akt-eNOS signaling activation and p38 MAPK inhibition. *(Anatol J Cardiol 2018; 20: 266-72)*

Keywords: ivabradine, angiogenesis, myocardial infarction, mice

Introduction

Myocardial infarction (MI) remains the most common cause of high mortality and a major impairment to quality of life worldwide (1). Pathologically, MI is defined as the loss of cardiomyocytes in the infarction area due to prolonged ischemia (2). Adverse left ventricular (LV) remodeling after MI due to necrosis, inflammation, cardiomyocyte hypertrophy, capillaries loss, and excessive fibrosis can eventually lead to heart failure (3, 4). Importantly, accumulative data have shown that insufficient myocardial capillary density and cardiac hypertrophy after MI are regarded as critical events in the process of cardiac remodeling (5, 6). Therefore, pro-angiogenesis and reducing cardiac hypertrophy are regarded as therapeutic approaches to restore the supply of nutrients and oxygen to the ischemic area and improve adverse LV remodeling after MI.

Ivabradine (IVA), a selective I(f) channel inhibitor affecting the sinus node, inhibits the pacemaker hyperpolarization-activated current and reduces the heart rate without any effect on inotropy, blood pressure, or the cardiac conduction system (7). Both the BEAUTIFUL and SHIFT trials have demonstrated the benefits of ivabradine (such as reducing cardiac morbidity and mortality) as a supplement to guideline-based treatment (such as β-blockers and angiotensin-converting enzyme inhibitors) in patients with LV dysfunction and with heart rates greater than 70 bpm. Therefore, in the 2012 European Society of Cardiology guidelines on heart failure, IVA was added to patients with chronic symptomatic systolic heart failure, with heart rates greater than 70 bpm, even if β-blockers were used (8, 9). A number of animal studies have documented the protective effect of IVA on LV remodeling after left anterior descending coronary artery ligation in mice or rats, and some possible mechanisms are

#X.W. and W.Y. contributed to equal work.

Address for correspondence: Shaoliang Chen MD, Division of Cardiology, Nanjing First Hospital, Nanjing Medical University; 68 Changle Rd, 210006 Nanjing-*China*

Phone: 86-025-52208048 E-mail: njsdxnk2017@163.com

Accepted Date: 31.07.2018 **Available Online Date:** 11.10.2018

DOI:10.14744/AnatolJCardiol.2018.46338

associated with a down-regulation of cardiac renin-angiotensin-aldosterone system transcripts, pro-angiogenesis, increase of sarcoplasmic reticulum Ca2+-ATPase (SERCA) activity, and reduction of functional hyperpolarization-activated cyclic nucleotide-gated (HCN) channels overexpression (10-12). However, the concrete mechanism of IVA on pro-angiogenesis in ischemic regions and regressing cardiac hypertrophy of the MI model is still elusive.

The activation of the phosphatidylinositol 3-kinase (PI3K) signaling pathway, including protein kinase B (Akt) and endothelial nitric oxide synthase (eNOS) phosphorylation, promotes nitric oxide (NO) production, which is essential for myocardial angiogenesis in MI models (13). Whether IVA could induce angiogenesis by increasing Akt-eNOS signaling activity in the heart after MI, thus restoring myocardial perfusion, remains largely unknown. p38 mitogen-activated protein kinase (MAPK) belongs to a stress-activated MAPKs family known to play a great role in multiple cellular signaling related to events, such as proliferation, growth, inflammation, injury, and apoptosis. Activation of p38 MAPK in the heart has been observed in MI-induced cardiac hypertrophy, and p38 MAPK inhibition provides cardio-protection against MI in mice (14).

Therefore, the aim of the study was to establish whether IVA promoted angiogenesis and reduced cardiac hypertrophy by enhancing Akt-eNOS signaling and suppressing p38 MAPK phosphorylation.

Methods

Experimental animal, MI model and treatment

Eight-week-old male C57BL/6 background mice were housed in groups with 12 h dark-light cycles and free access to food and water. These conditions are in accordance with the Guide for the Care and Use of Laboratory Animals published by the US National Institutes of Health (NIH publication no. 85-23, revised in 1996), and the regulations on mouse welfare and ethics of Nanjing University. The animal protocol (YZZ25) was reviewed and approved by the Ethics Committee of Model Animal Research Center of Nanjing University. Cervical dislocation was a method to provide the mouse with a fast and painless death.

MI was generated following a method reported previously in mice with slight modifications (15). Briefly, mice were anesthetized intraperitoneally with pentobarbital sodium (30–50 mg/kg). A 20-gauge polyethylene catheter was intubated into the trachea and a volume-cycled rodent respirator (model 683; Harvard Apparatus, Holliston, MA, USA) provided positive pressure ventilation at 2-3 ml/cycle and a respiratory rate of 120 cycles/min. After the thoracic cavity at the level of the fourth rib and along the left sternal border was opened, the left anterior descending coronary artery (LAD) was ligated with a 7-0 silk suture 3 mm from the tip of the left auricle. The chest wall was closed with a continuous 6-0 prolene suture, followed by a 4-0 polyester suture in order to close the skin. The procedure of sham operation was the same as the above-mentioned MI induction but without LAD ligation. After LAD ligation in mice, ST segment elevation in the chest leads checked by an electrocardiogram (ECG) was the sign of a successful MI surgery and the success rate was 87.5%. The mortality of these mice after surgery in our study was 95% due to cardiac rupture.

Ivabradine (Servier, Courbevoie, France) was dissolved into phosphate buffer solution (PBS). Nineteen mice were randomly assigned into three groups as follows: sham group (without LAD occlusion and only receiving an intragastric gavage of 10 ml/kg/day PBS, n=6), model group (LAD ligation and receiving an intragastric gavage of 10 ml/kg/day PBS, n=6) and ivabradine group (LAD ligation and receiving an intragastric gavage of ivabradine at the dose of 10 mg/kg/day, n=7). Furthermore, all groups were administered accordingly for four weeks.

Cardiac function assessment by echocardiography

An echocardiographic examination was performed on day 30 following the MI induction using a Vevo 2100 (Visual Sonics, Toronto, Canada), equipped with a 30-MHz transducer, which was used for noninvasive transthoracic echocardiography. Two-dimensional guided M-mode tracings were recorded. The internal diameter of the LV in the short-axis plane was measured at the end diastole and the end systole from M-mode recordings were taken just below the tips of the mitral valve leaflets. After measurement, LV internal diameter at end-diastole (LVIDD) as indicative of cardiac diastolic function were measured. Two indexes of cardiac systolic function, including LV fractional shortening (LVFS) and LV ejection fraction (LVEF), were calculated.

Heart rate measurement

Mice were anesthetized with sodium pentobarbital, and ECG was continuously recorded before and 30 minutes after injection. In accordance with the principle of electrocardiogram, four electrodes were inserted into the subcutaneous tissue of the mice limbs, and then the signals were recorded on a four channel direct-writing oscillograph (ALC MPA, Shanghai Alcott Biotech Co., Ltd., China), digitally sampled system (1 kHz), and on a personal computer equipped with an analog to digital interface.

Western blot analysis

Western blot analyses were performed as previously reported (16). Heart tissues of mice were dissected and snap-frozen in liquid nitrogen until the time of use. Tissue lysates of mice were prepared in lysis buffer (20 mM Tris, 150 mM NaCl, 10% glycerol, 20 mM glycerophosphate, 1% NP40, 5 mM ethylenediaminetetraacetic acid (EDTA), 0.5 mM ethylenebis (oxyethylenenitrilo) tetraacetic acid (EGTA), 1 mM Na_3VO_4, 0.5 mM phenylmethanesulfonyl fluoride (PMSF), 1 mM benzamidine, 1 mM DL-Dithiothreitol (DTT), 50 mM NaF, 4 μM leupeptin, pH=8.0). Equal amounts of total proteins (50 μg) were resolved by 10% sodium dodecyl sulfate-polyacrylamide gel electrophoresis (SDS-PAGE) and transferred to polyvinylidene fluoride (PVDF) membranes (Millipore, Billerica, MA, USA). Membranes were blocked with 5% non-fat

Anatol J Cardiol 2018; 20: 266-72
DOI:10.14744/AnatolJCardiol.2018.46338

milk in Tris Buffered saline Tween (TBST) (50 mM Tris, 150 mM NaCl, 0.5 mM Tween-20, pH=7.5) and then incubated overnight with primary antibodies. Total Akt, phospho-Akt (Thr308), phospho-Akt (Ser473), p38, and phospho-p38 MAPK (Thr180/Tyr182) were purchased from Cell Signaling Technology (CST, Danvers, MA, USA). Phospho-eNOS (Ser1177) and phospho-eNOS (Thr 495) were produced from Santa Cruz Biotechnology Inc. (Dallas, Texas, USA). eNOS and HRP-linked secondary antibodies were purchased from BD bioscience (Bedford, MA, USA) and Thermos Scientific (Pittsburgh, PA, USA), respectively. Image J software (NIH) was used to perform densitometric analysis.

Histology and immunofluorescence staining

The protocols of Masson's staining and immunofluorescence (IF) were performed as described previously (17). Briefly, heart samples were first washed with ice-cold PBS and then fixed in 4% paraformaldehyde at 4 °C. The samples were processed successively by (a) a 30min washing in PBS at 4 °C; (b) 15 min each in 30%, 50%, 75%, and 85% ethanol, and then 2×10 min of incubation in 95% and 100% ethanol at room temperature (RT); (c) 3×10 min of incubation in xylene at RT; (d) 20 min of incubation in paraffin/xylene (1:1) at 65 °C; and (e) 3×30 min of incubation in fresh paraffin at 65 °C. The processed samples were embedded in paraffin and sectioned to a thickness of 6 μm, and then the sections were stained. At the beginning of the lower left atrial appendage, the heart was sectioned every 600 μm from bottom to top. The fibrotic area to the whole left ventricle area ratio in a section was calculated, and averaged after measuring 4 sections.

IF staining was performed using anti-wheat germ agglutinin (WGA) (Abcam) and anti-CD31 (BD bioscience) antibodies at 4°C overnight. Fluorescence microscopy images were obtained with a Research Fluorescence Microscope (Olympus America Inc., Center Valley, PA, USA) equipped with a digital camera. Images were collected and recorded by using Adobe Photoshop® 5.0 (Adobe Systems Inc., San Jose, CA, USA) on an IBM R52 computer (IBM, Armonk, NY, USA). Area of cardiomyocytes and number of capillaries were measured with 400× magnification, and averaged after determining in 5 high-power fields.

Statistical analysis

Data are presented as means±SD values. Statistical analyses were performed using SPSS version 20 (SPSS Inc., Chicago, Illinois, USA). For comparisons between two groups, statistical significance was determined using the unpaired two-tailed Student's t-test. One-way ANOVA was applied for multiple comparisons and Tukey's post-hoc test was used between two groups

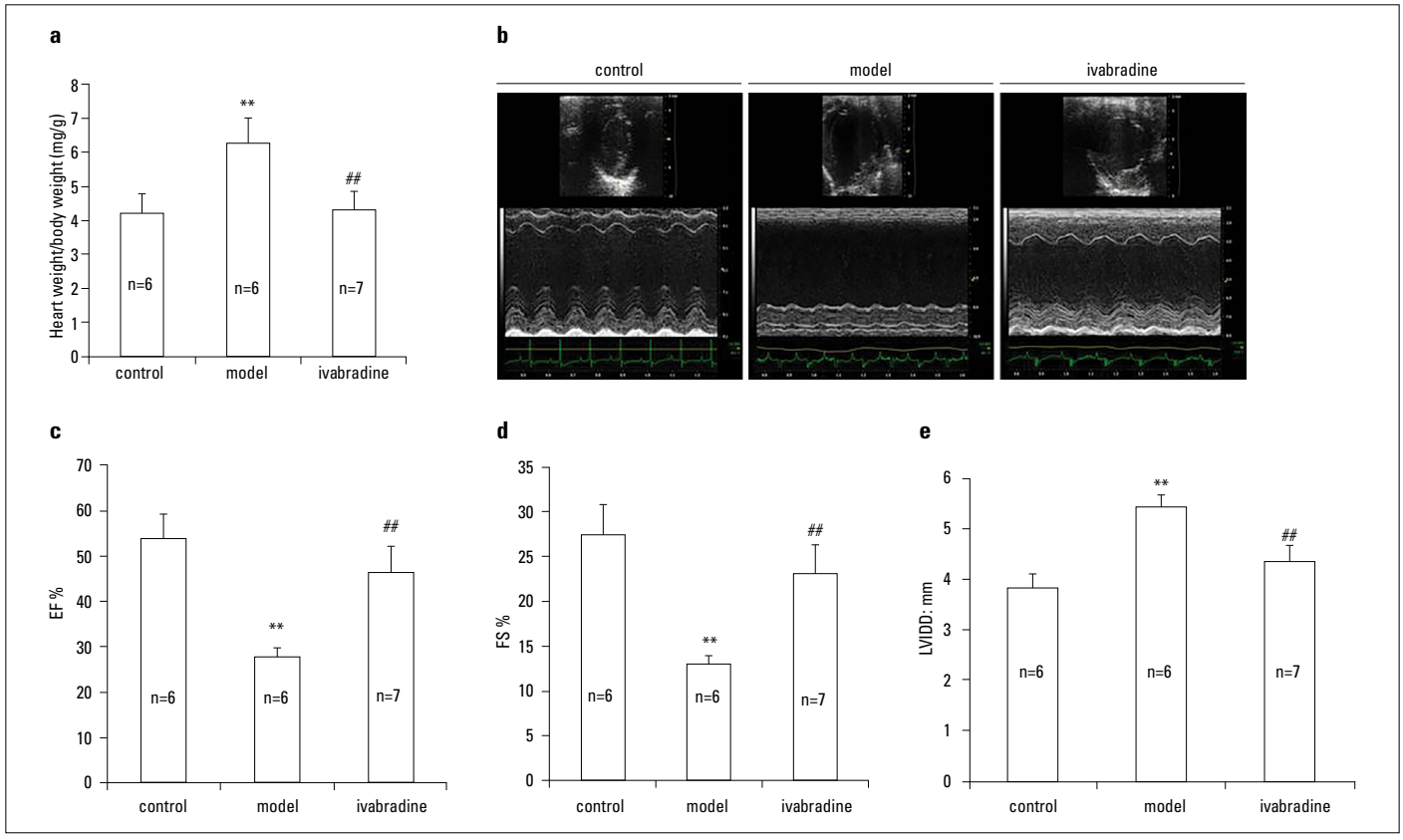

Figure 1. Effects of IVA on heart weight/body weight ratio and cardiac function in MI mice.
(a) Ratio of heart weight to body weight. (b-e) Echocardiography measurement. IVA- ivabradine; MI- myocardial infarction; EF- ejection fraction; FS- fractional shortening; LVIDD- left ventricular internal diastolic diameter; control, mice after sham operation; model, mice with left descending coronary artery (LAD) ligation; ivabradine, mice with LAD ligation treated with IVA. Data are given as means±SEM. $^{**}P<0.01$ vs. control group, $^{\#\#}P<0.01$ vs. model group

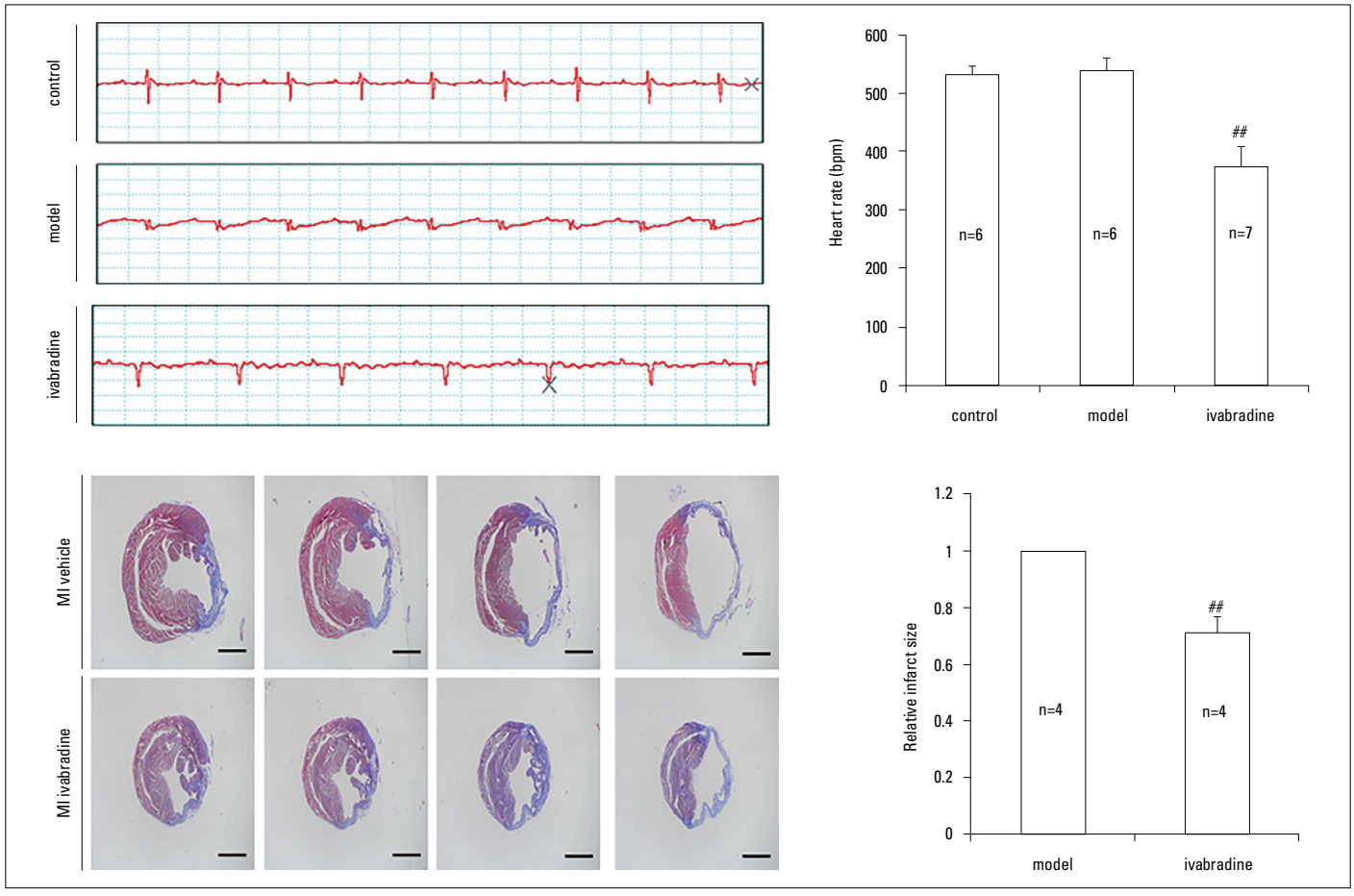

Figure 2. Effects of IVA on heart rate and cardiac fibrotic area in MI mice.
(a) Electrocardiogram recorded. Time scale: 50 ms/cell; (b) Heart rate measurement; (c) Masson's staining was used to display fibrotic areas (in blue). Scale bar: 1.25 mm; (d) Quantitation of fibrotic area (n=4). Data are given as means±SEM. $^{##}P<0.01$ vs. model group

following a $p<0.05$ of one-way ANOVA. A $p<0.05$ was considered statistically significant.

Results

Effects of IVA on heart weight/body weight ratio and cardiac function in MI mice

Among the three groups, the model group was not treated with IVA and the heart weight/body weight ratio in this group was the highest, indicating heart hypertrophy provoked by MI ($p<0.001$). Treatment with IVA for 4 weeks significantly suppressed cardiac hypertrophy after MI, as indicated by the heart weight/body weight ratio ($p<0.001$) (Fig. 1a).

At 4 weeks after MI, heart systolic function was considerably impaired, as indicated by the LVEF and LVFS measurements ($p<0.001$). Treatment with IVA greatly improved cardiac systolic function at 4 weeks after MI ($p<0.001$) (Fig. 1b, 1c, 1d). An increase in LVIDD is an index for cardiac dilation. LVIDD was highest in the model group, but was significantly smaller in the IVA group ($p<0.001$) (Fig. 1b, 1e).

Taken together, these results indicated that IVA alleviated heart hypertrophy and improved heart dysfunction after MI.

Effects of IVA on heart rate and cardiac fibrotic area in MI mice

After surgery-induced MI, mice with MI had no significant change in heart rate as showed in ECG compared to that of the sham group ($p>0.05$). 4 weeks after IVA medication in MI mice, the heart rate and fibrotic area were declined notably compared to those of the model group ($p<0.001$), indicating that IVA produced the results of heart rate reduction and decreased cardiac fibrosis in MI mice (Fig. 2a, 2b, 2c, 2d).

Effects of IVA on cardiomyocyte hypertrophy and capillary density in MI mice

At 4 weeks after MI, the structure of cardiomyocytes was disarrayed, and the size of cardiomyocytes increased significantly in the left ventricle of vehicle-treated mice compared with sham mice ($p<0.001$). After treatment with IVA, the increase in cardiomyocyte size was less in IVA-treated mice than vehicle-treated MI mice ($p<0.001$) (Fig. 3a, 3b).

Anatol J Cardiol 2018; 20: 266-72
DOI:10.14744/AnatolJCardiol.2018.46338

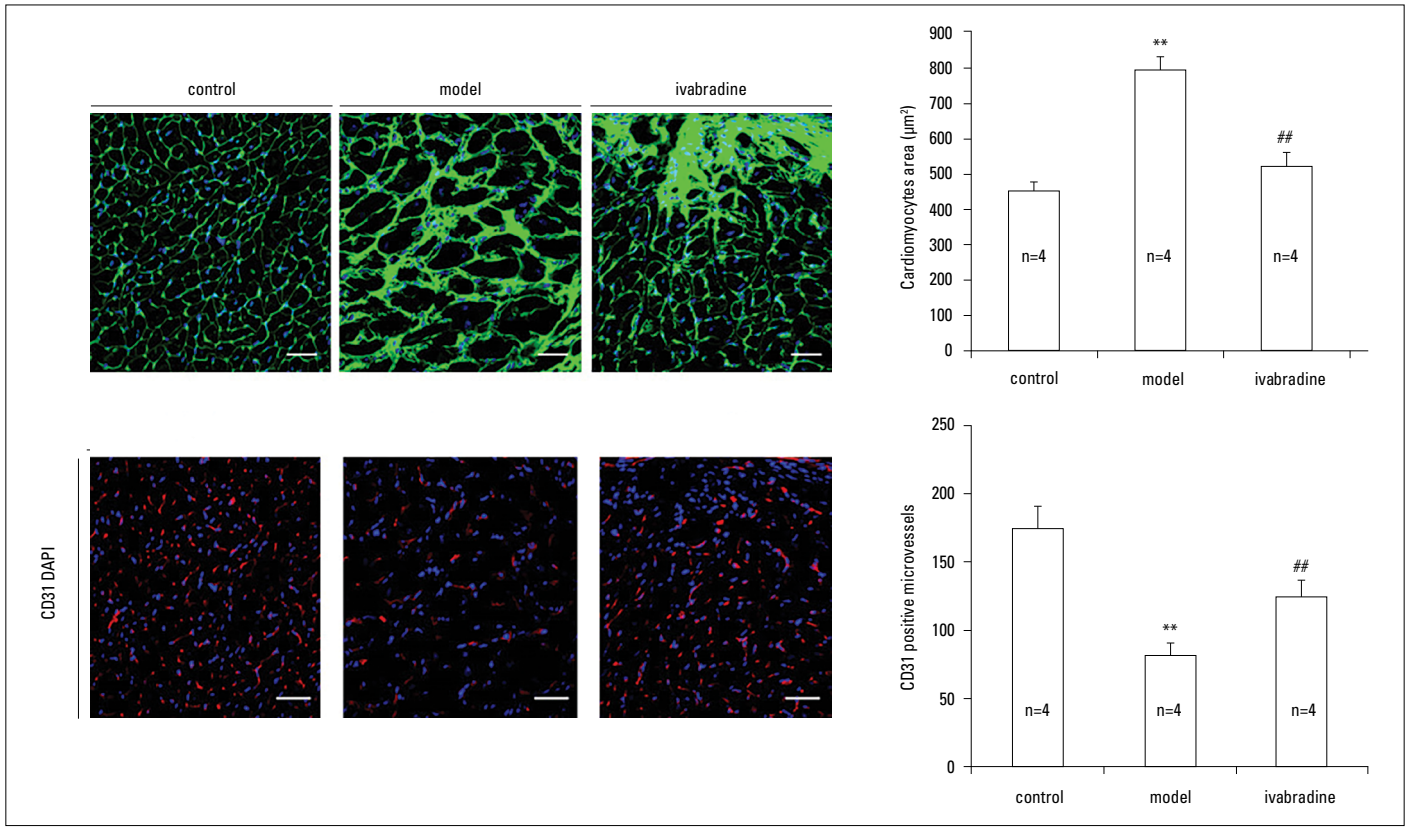

Figure 3. Effects of IVA on cardiomyocyte hypertrophy and capillary density in MI mice.
(a) Wheat germ agglutinin staining was used to display the structure and size of cardiomyocytes. Sections were from papillary muscle. Scale bar: 40 μm; (b) Quantitation of cross areas of cardiomyocytes (n=4); (c) CD31 staining was used to show capillary density. Scale bar: 40 μm; (d) Quantitation of capillary density (n=4). Data are given as means±SEM. ** P<0.01 vs. control group, ## P<0.01 vs. model group

We examined capillary density by using a CD31 assay among these three groups. The results showed that capillary density decreased notably in mice of the model group compared with mice of the sham group (p<0.001). However, IVA administration substantially increased capillary formation (p=0.002) (Fig. 3c, 3d).

In total, these results showed that IVA can reduce cardiomyocyte hypertrophy and promote angiogenesis in MI mice.

Effects of IVA on Akt-eNOS signaling and p38 MAPK phosphorylation in the hearts of MI mice

To further investigate the possible molecular mechanism by which IVA promoted heart angiogenesis and improved cardiac remodeling, we examined Akt-eNOS pathway and p38 MAPK phosphorylation. After MI for 4 weeks, there were no differences in the phosphorylation of Akt Thr308 and Ser 473 nor in the phosphorylation of eNOS Thr 495 and Ser 1177 in the hearts of MI mice as compared to those in sham-operation mice (p>0.05). However, activation of p38 MAPK, as indicative of the marked increase in its phosphorylation, was observed in the hearts of MI mice (p=0.002). IVA administration can significantly increase the phosphorylation of Akt Thr308, Akt Ser 473, and eNOS Ser 1177 in the hearts of mice with MI (p=0.002, p<0.001, p=0.005), whereas the phosphorylation of eNOS Thr 495 in IVA-treated mice declined slightly in comparison with as mice of the model group (p>0.05). Furthermore, chronic IVA treatment resulted in significantly reduced p38 MAPK activation (as measured by its phosphorylation) in post-MI mouse myocardium (p=0.009) (Fig. 4a, 4b).

In conclusion, chronic IVA medication can enhance Akt-eNOS signaling and inhibit p38 MAPK phosphorylation in the hearts of MI mice.

Discussion

It has been reported that early and late heart rate (HR) reduction by IVA significantly increases the capillary to myocyte ratio and promotes cardiac angiogenesis in MI rats (12). However, the possible mechanism is still unknown. In the present study, we showed that IVA, a pure HR reducing agent, markedly improved cardiac dysfunction and adverse remodeling after MI in the mice. A potential mechanism of this effect can be that IVA promoted angiogenesis through enhancing Akt-eNOS signaling in the hearts of mice with MI.

Angiogenesis is defined as the formation of new blood vessels from pre-existing vessels, which plays a protective role in the adverse cardiac remodeling of MI (18, 19). Angiogenesis is a compensatory response that re-establishes the blood supply

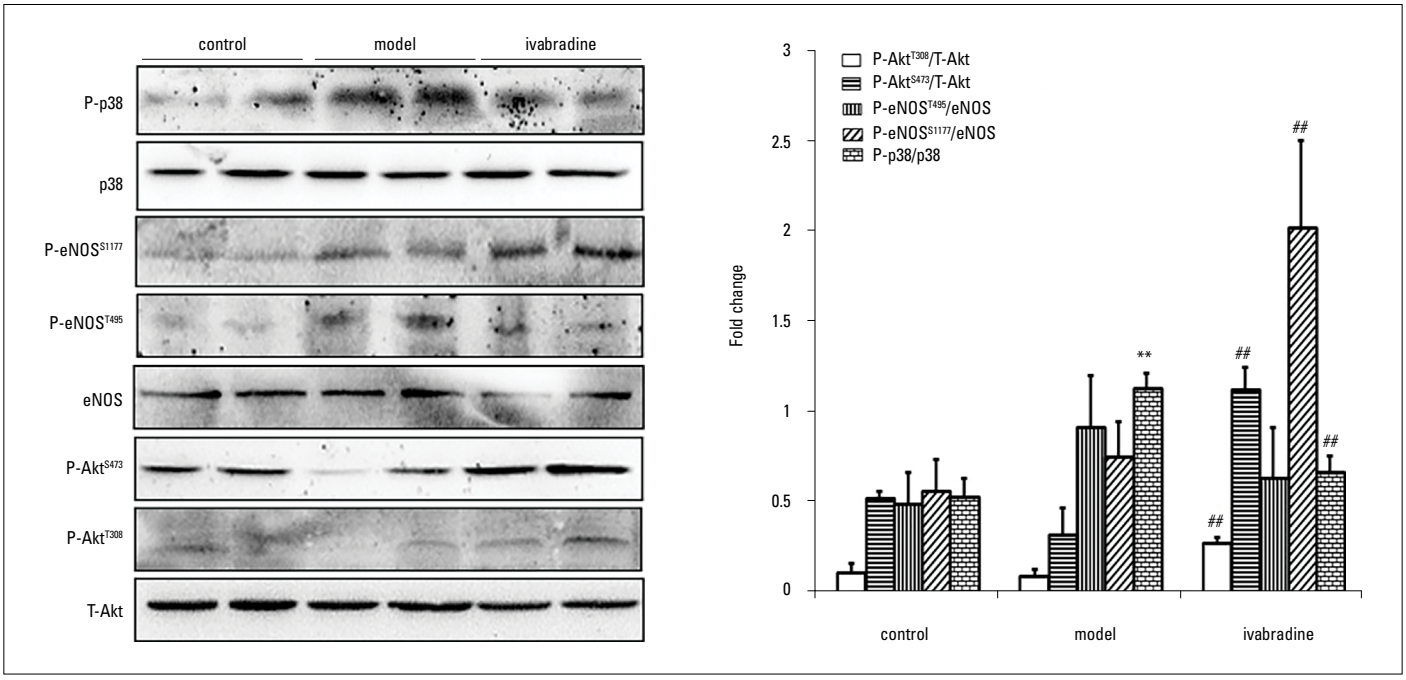

Figure 4. Effects of IVA on Akt-eNOS signaling and p38 MAPK phosphorylation in heart of MI mice.
(a) Western blot analysis of Akt, eNOS, and p38 MAPK phosphorylation in heart tissues of MI mice. (b) Quantitative study (n=4). Akt- protein kinase B; eNOS- endothelial nitric oxide synthase; p38 MAPK- p38 mitogen-activated protein kinase. Data are given as means±SEM. $^{**}P<0.01$ vs. control group, $^{\#\#}P<0.01$ vs. model group

to the cardiac ischemic area. The promotion of angiogenesis has been accepted as a promising therapeutic method for MI. In an ischemic heart, angiogenesis mainly depends on the vascular endothelial growth factor (VEGF) expression (20). The angiogenic response to VEGF is mainly mediated by eNOS, which is activated by the PI3K/Akt signaling. Akt is a serine/threonine protein kinase recruited to the cell membrane by its binding to PI3K-produced phosphoinositides. At that time, Akt is phosphorylated and activated, which leads to the eventual activation of eNOS (21). The phosphorylation of the Ser 1177 residue increases eNOS activity, whereas the Thr 495 residue phosphorylation has the opposite effect (22). In this study, we found that the phosphorylation of Akt Thr308, Akt Ser 473, and eNOS Ser 1177 was increased by chronic IVA administration of myocardium to mice with MI, indicating that IVA's promotion of angiogenesis was closely associated with its property of Akt-eNOS signal activation. It has been shown that IVA reduces oxidative stress, improves endothelial function, and prevents atherosclerosis in the aorta of apolipoprotein E-deficient mice, but IVA does not alter levels of phosphorylated endothelial nitric oxide synthase or of Akt (23). Furthermore, Thuillez and his team have reported that IVA improves diastolic LV function, increases LV microvessel density, improves acetylcholine-induced relaxation of coronary arteries and flow-induced vasodilatation of mesenteric resistance arteries, and normalizes chronic heart failure-related decreased eNOS expression of mesenteric arteries in rats with LAD ligation (24). However, different disease models and/or organs may be responsible for the different results in our study.

It has been demonstrated that eNOS gene transfer improves ventricular remodeling through inhibition of MAPK signaling after myocardial infarction in rats, whereas the protective effects of eNOS were blocked by N(ω)-nitro-L-arginine methyl ester (L-NAME) administration and p38MAPK phosphorylation was significantly abrogated by L-NAME (25). In the heart, p38 MAPK activation has been observed in mice with pressure overload or MI-induced cardiac hypertrophy. In addition, inhibition of p38 MAPK reportedly protected against myocardial injury (14, 26). Yang et al. (13) have reported that activation of the p38 MAPK signaling pathway is observed in the hearts of chronic viral myocarditis mice as compared to normal mice, and IVA achieves cardio-protection through attenuating the P-p38 expression (27). In our study, we can also conclude that cardio-protection of IVA was attributed to significantly reducing p38 MAPK phosphorylation of myocardium in post-MI mice, partially due to Akt-eNOS signaling activation.

Study limitation

The small sample size of our study is a limitation. Further studies are required to elucidate the precise mechanisms underlying how IVA promotes angiogenesis in mice with MI.

Conclusion

In summary, IVA can perform the two functions of promoting angiogenesis and reducing cardiac hypertrophy, which were closely associated with Akt-eNOS signaling activation and p38 MAPK inhibition.

Anatol J Cardiol 2018; 20: 266-72
DOI:10.14744/AnatolJCardiol.2018.46338

Acknowledgement: This work was supported by the National Natural Science Foundation of China (grant number 81600296).

Conflict of interest: None declared.

Peer-review: Externally peer-reviewed.

Authorship contributions: Concept – X.W., S.C.; Design – X.W.; Supervision – F.Y.; Fundings – X.W., S.C.; Materials – X.W., W.Y.; Data collection &/or processing – X.W., W.Y.; Analysis &/or interpretation – X.W., W.Y.; Literature search – Z.W.; Writing – X.W.; Critical review – F.Y., S.C.

References

1. Benjamin EJ, Blaha MJ, Chiuve SE, Cushman M, Das SR, Deo R, et al.; American Heart Association Statistics Committee and Stroke Statistics Subcommittee. Heart Disease and Stroke Statistics-2017 Update: A Report From the American Heart Association. Circulation 2017; 135: e146-e603. [CrossRef]
2. Jennings RB, Ganote CE. Structural changes in myocardium during acute ischemia. Circ Res 1974; 35 (Suppl 3): 156-72.
3. Anzai T. Post-infarction inflammation and left ventricular remodeling: a double-edged sword. Circ J 2013; 77: 580-7. [CrossRef]
4. Niizeki T, Takeishi Y, Arimoto T, Takahashi H, Shishido T, Koyama Y, et al. Cardiac-specific overexpression of diacylglycerol kinase zeta attenuates left ventricular remodeling and improves survival after myocardial infarction. Am J Physiol Heart Circ Physiol 2007; 292: H1105-12.
5. Van Kerckhoven R, van Veghel R, Saxena PR, Schoemaker RG. Pharmacological therapy can increase capillary density in post-infarction remodeled rat hearts. Cardiovasc Res 2004; 61: 620-9. [CrossRef]
6. Yoshida K, Yasujima M, Casley DJ, Johnston CI. Effect of Chronic Neutral Endopeptidase Inhibition on Cardiac Hypertrophy after Experimental Myocardial Infarction. Jpn Circ J 1998; 62: 680-6. [CrossRef]
7. Mackiewicz U, Gerges JY, Chu S, Duda M, Dobrzynski H, Lewartowski B, et al. Ivabradine protects against ventricular arrhythmias in acute myocardial infarction in the rat. J Cell Physiol 2014; 229: 813-23.
8. O'Connor DM, Smith RS, Piras BA, Beyers RJ, Lin D, Hossack JA, et al. Heart Rate Reduction with Ivabradine Protects against Left Ventricular Remodeling by Attenuating Infarct Expansion and Preserving Remote-Zone Contractile Function and Synchrony in a Mouse Model of Reperfused Myocardial Infarction. J Am Heart Assoc 2016; 5. pii: e002989. [CrossRef]
9. McMurray JJ, Adamopoulos S, Anker SD, Auricchio A, Böhm M, Dickstein K, et al.; ESC Committee for Practice Guidelines. ESC Guidelines for the diagnosis and treatment of acute and chronic heart failure 2012: The Task Force for the Diagnosis and Treatment of Acute and Chronic Heart Failure 2012 of the European Society of Cardiology. Developed in collaboration with the Heart Failure Association (HFA) of the ESC. Eur Heart J 2012; 33: 1787-847. [CrossRef]
10. Maczewski M, Mackiewicz U. Effect of metoprolol and ivabradine on left ventricular remodelling and Ca2+ handling in the post-infarction rat heart. Cardiovasc Res 2008; 79: 42-51. [CrossRef]
11. Christensen LP, Zhang RL, Zheng W, Campanelli JJ, Dedkov EI, Weiss RM, et al. Postmyocardial infarction remodeling and coronary reserve: effects of ivabradine and beta blockade therapy. Am J Physiol Heart Circ Physiol 2009; 297: H322-30. [CrossRef]
12. Ulu N, Henning RH, Goris M, Schoemaker RG, van Gilst WH. Effects of ivabradine and metoprolol on cardiac angiogenesis and endothelial dysfunction in rats with heart failure. J Cardiovasc Pharmacol 2009; 53: 9-17. [CrossRef]
13. Yang C, Talukder MA, Varadharaj S, Velayutham M, Zweier JL. Early Ischaemic Preconditioning Requires Akt- and Pka-Mediated Activation of Enos Via Serine1176 Phosphorylation. Cardiovasc Res 2013; 97: 33-43. [CrossRef]
14. Liu YH, Wang D, Rhaleb NE, Yang XP, Xu J, Sankey SS, et al. Inhibition of p38 mitogen-activated protein kinase protects the heart against cardiac remodeling in mice with heart failure resulting from myocardial infarction. J Card Fail 2005; 11: 74-81. [CrossRef]
15. Matsumoto K, Ogawa M, Suzuki J, Hirata Y, Nagai R, Isobe M. Regulatory T lymphocytes attenuate myocardial infarction-induced ventricular remodeling in mice. Int Heart J 2011; 52: 382-7. [CrossRef]
16. Sato A, Suzuki S, Watanabe S, Shimizu T, Nakamura Y, Misaka T, et al. DPP4 Inhibition Ameliorates Cardiac Function by Blocking the Cleavage of HMGB1 in Diabetic Mice After Myocardial Infarction. Int Heart J 2017; 58: 778-86. [CrossRef]
17. Gao J, Liu X, Wang B, Xu H, Xia Q, Lu T, et al. Farnesoid X receptor deletion improves cardiac function, structure and remodeling following myocardial infarction in mice. Mol Med Rep 2017; 16: 673-9. [CrossRef]
18. Wiley DM, Kim JD, Hao J, Hong CC, Bautch VL, Jin SW. Distinct signalling pathways regulate sprouting angiogenesis from the dorsal aorta and the axial vein. Nat Cell Biol 2011; 13: 686-92. [CrossRef]
19. Chen K, Yan M, Li Y, Dong Z, Huang D, Li J, et al. Intermedin1-53 enhances angiogenesis and attenuates adverse remodeling following myocardial infarction by activating AMP-activated protein kinase. Mol Med Rep 2017; 15: 1497-506. [CrossRef]
20. Fukumura D, Gohongi T, Kadambi A, Izumi Y, Ang J, Yun CO, et al. Predominant role of endothelial nitric oxide synthase in vascular endothelial growth factor-induced angiogenesis and vascular permeability. Proc Natl Acad Sci U S A 2001; 98: 2604-9. [CrossRef]
21. Kawasaki K, Smith RS Jr, Hsieh CM, Sun J, Chao J, Liao JK. Activation of the phosphatidylinositol 3-kinase/protein kinase Akt pathway mediates nitric oxide-induced endothelial cell migration and angiogenesis. Mol Cell Biol 2003; 23: 5726-37. [CrossRef]
22. Fleming I, Busse R. Molecular mechanisms involved in the regulation of the endothelial nitric oxide synthase. Am J Physiol Regul Integr Comp Physiol 2003; 284: R1-12. [CrossRef]
23. Custodis F, Baumhäkel M, Schlimmer N, List F, Gensch C, Böhm M, et al. Heart rate reduction by ivabradine reduces oxidative stress, improves endothelial function, and prevents atherosclerosis in apolipoprotein E-deficient mice. Circulation 2008; 117: 2377-87. [CrossRef]
24. Fang Y, Debunne M, Vercauteren M, Brakenhielm E, Richard V, Lallemand F, et al. Heart rate reduction induced by the if current inhibitor ivabradine improves diastolic function and attenuates cardiac tissue hypoxia. J Cardiovasc Pharmacol 2012; 59: 260-7. [CrossRef]
25. Chen LL, Zhu TB, Yin H, Huang J, Wang LS, Cao KJ, et al. Inhibition of MAPK signaling by eNOS gene transfer improves ventricular remodeling after myocardial infarction through reduction of inflammation. Mol Biol Rep 2010; 37: 3067-72. [CrossRef]
26. Hayashida W, Kihara Y, Yasaka A, Inagaki K, Iwanaga Y, Sasayama S. Stage-specific differential activation of mitogen-activated protein kinases in hypertrophied and failing rat hearts. J Mol Cell Cardiol 2001; 33: 733-44. [CrossRef]
27. Yue-Chun L, Guang-Yi C, Li-Sha G, Chao X, Xinqiao T, Cong L, et al. The Protective Effects of Ivabradine in Preventing Progression from Viral Myocarditis to Dilated Cardiomyopathy. Front Pharmacol 2016; 7: 408.